Interfacial Phenomena Controlling Particle Morphology of Composite Latexes

YI-CHERNG CHEN, VICTORIA DIMONIE, and MOHAMED S. EL-AASSER

Emulsion Polymers Institute, Center for Polymer Science and Engineering and Department of Chemical Engineering, Lehigh University, Bethlehem, Pennsylvania 18015

SYNOPSIS

A thermodynamic analysis and a mathematical model were derived to describe the free energy changes corresponding to various possible morphologies in composite latex particles. Seeded batch emulsion polymerization was carried out at 70°C using as seed monodisperse polystyrene latex particles having different surface polarity. The surface polarity was estimated by contact angle measurement at the latex "film"/water interface for octane as the probe liquid. Methyl methacrylate and ethyl methacrylate were polymerized in a second stage seeded emulsion polymerization using polystyrene particles as seed in the presence of a nonionic stabilizer, nonyphenol polyethylene oxide (Igepal Co-990). Two types of initiators, potassium persulfate ($K_2S_2O_8$) and azobisiobutyronitrile (AIBN), were used to change the interfacial tension between the second stage polymer (in monomer) and water interface. The values of the interfacial tension of polymer solutions in the second stage monomer vs. the aqueous phase, measured by drop-weight–volume method under conditions similar to those prevailing during the polymerization, correlated well with the determined particle surface polarity and the observed TEM particle morphology. The results showed that, rather than the polymer bulk hydrophilicity, the surface particle polarity is the controlling parameter in deciding which phase is inside or outside in the composite particle. The variation of the polymer phase interfacial tension with polymer concentration was also estimated. Based on experimentally measured interfacial tensions, composite particle configurations were predicted. The predicted morphologies showed good agreement with the observed particle morphologies of the composite latexes.

INTRODUCTION

Control of composite latex particle morphology is important for many latex applications such as adhesives, coatings, impact modification, and toughening of polymer matrices. Many of the polymerization parameters and conditions are known to affect the particle morphology. For example: water solubility of the monomers; type, amount, and addition mode of other ingredients such as emulsifier, initiator, chain transfer, or crosslinking agents; degree of compatibility of polymers; viscosity of the polymerization loci; degree of grafting of the second stage polymer onto the core particle; polarity of the seed particle; the interfacial tension of boundary phases; methods of monomer addition; and polymerization temperature. Depending on the polymerization parameters and conditions, a variety of particles of different morphological features, ranging from the familiar core–shell[1-4] and "inverted" core–shell[4-6] to phase separated structures such as sandwich structures,[4] hemispheres,[4,7] "raspberry-like,"[8,9] and void particles,[10,11] have been prepared by seeded emulsion polymerization techniques. However, there is no systematic way which is available to control and predict the particle morphology based on the operating parameters in the emulsion polymerization process. Recently, Sundberg et al.[12,13] presented a thermodynamic analysis of the morphology of polymer encapsulated oil droplets. Their analysis revealed that the interfacial tension of each phase is a key factor governing the type of microcapsules formed (core–shell, hemispheres, or individual par-

Journal of Applied Polymer Science, Vol. 42, 1049–1063 (1991)
 CCC 0021-8995/91/041049-15$04.00

ticles). For the composite polymer particles, Dimonie et al.[14] supported experimentally the hypothesis that in addition to the viscosity of the polymerization locus (related to the chain mobility), the interfacial tension of the polymer phases is one of the main parameters controlling the particle morphology. The purpose of this paper is to quantitatively describe the effect of interfacial tension on the morphology of composite latex based on a thermodynamic analysis.

THERMODYNAMIC CONSIDERATIONS

In the case of two-step emulsion polymerization of incompatible polymers which tend to phase separate, the development of final morphology in a composite latex particle involves the movement, or diffusion of at least two molecular species under the influence of some driving force. In order to concentrate upon the driving force, i.e., the Gibbs free energy change of the process, the overall resistance to diffusion within the particle during morphology development will not be considered at this moment.

The thermodynamic analysis which will be considered for determining the latex particle morphology is based on the approach presented 20 years ago by Torza and Mason.[15] They studied the interfacial behavior of systems containing three mutually immiscible liquids and examined the conditions necessary for a coacervate droplet (liquid 3) to engulf an initial droplet (liquid 1) when both are immersed in a continuous phase (liquid 2) by the spreading coefficient, S, which is defined as

$$S_i = \gamma_{jk} - (\gamma_{ij} + \gamma_{ik}) \qquad (1)$$

By assuming that the interfacial tension of liquid 1 against liquid 2 (γ_{12}) is greater than that of liquid 3 against liquid 2 (γ_{23}), only three possible sets of values for S exist. These correspond to three different equilibrium configurations: complete engulfing (core–shell), partial engulfing (hemisphere), and nonengulfing (individual particle). Complete engulfing occurs only if $S_3 > 0$, $S_2 < 0$, and $S_1 < 0$. On the other hand, when $S_2 < 0$, $S_3 < 0$, and $S_1 < 0$ the partial engulfing was preferred. Torza and Mason[15] demonstrated the general validity of their approach by making a number of interfacial tension measurements, calculating values of S, and then observing what occurred in an actual three-phase system. In most cases, prediction of engulfing based on S were satisfactory. Sundberg et al.[12] applied Torza and Mason's approach to determine the various morphologies involved in the polymer encapsulation of a relatively large size oil droplet in the millimeter range.

Our thermodynamic analysis is similar to that presented by Sundberg et al.[12] for the polymer encapsulation of oil droplet by considering the free energy changes for the following hypothetical pathways. In our analysis, the particles are in the submicron range. The initial state consists of a pure polymer phase 1 (preformed polymer) suspended in water containing some surfactant, and another completely separated bulk phase of pure polymer 2 (postformed polymer). The final state is one of the morphologies shown in Figure 1.

It is assumed that no mixing or demixing is involved. The only contribution to the free energy change for this pathway is the criterion of new interfaces. For latex particles dispersed in a continuous water phase, those interfaces include polymer 1/water, polymer 2/water, and polymer 1/polymer 2.

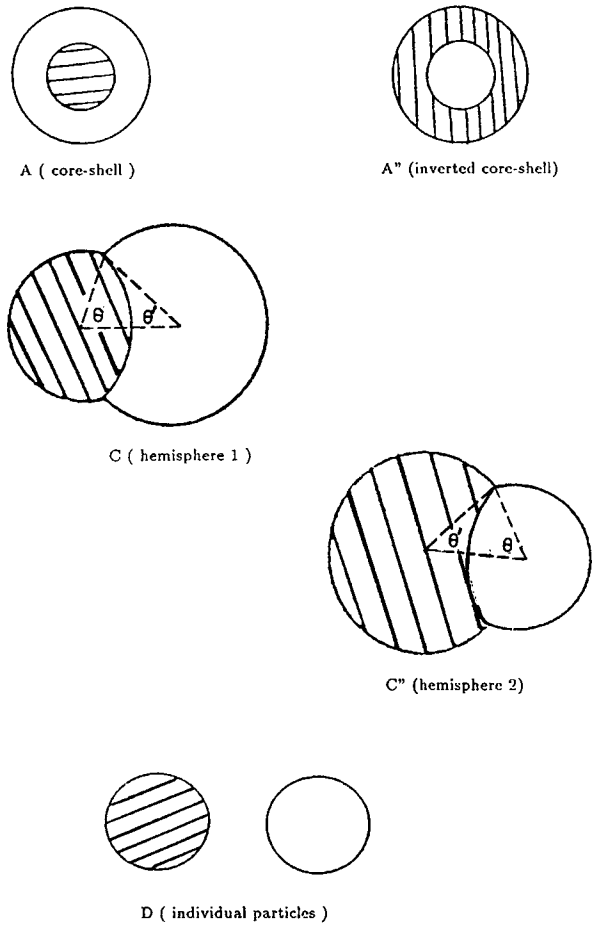

Figure 1 Various morphological structures of particles dispersed in water. ▨: polymer 1; □: polymer 2.

The total free energy change for all types of configurations shown in Figure 1 can be expressed as

$$\Delta G = \sum \gamma_{ij} A_{ij} - \gamma_{op1w} A'_o \qquad (2)$$

where γ_{ij} is the interfacial tension between i and j and A_{ij} is the corresponding interfacial area. Each of the morphologies shown in Figure 1 has different combinations of $\gamma_{ij}A_{ij}$, depending on their geometric feature. γ_{op1w} is the interfacial tension of original polymer 1 (containing surfactant, if present) suspended in water and A'_o is its interfacial area. The thermodynamically preferred morphology will be the one which has the minimum interfacial free energy change. This approach is feasible if all of the γ_{ij} can be measured independently. It should be noted that the practical need of stabilizing agents and initiator may greatly affect the interfacial tension at the polymer/water interface and, therefore, particle morphology.

The free energy change for case A (polymer 1 as the core, polymer 2 as the shell) is

$$\Delta G = \gamma_{12} A_{12} + \gamma_{2w} A_{2w} - \gamma_{op1w} A'_o \qquad (3)$$

or

$$\Delta G = \gamma_{12} 4\pi R_c^2 + \gamma_{2w} 4\pi R^2 - \gamma_{1w} 4\pi R_c^2 \qquad (4)$$

where the interfacial tensions are those between the two polymers, γ_{12}; polymer 1 and water, γ_{1w}; and polymer 2 and water, γ_{2w}. R_c is the radius of the core, i.e., polymer 1, and R is that of the overall composite particle. In this particular case, $R_c = R_1$ and $R = R_2$. R_1 and R_2 are the radii of polymer 1 and polymer 2, respectively. If we define the volume ratio V_r as

$$V_r = (R/R_c)^3 - 1 \qquad (5)$$

then the above expression can be simplified to

$$\Delta\psi = \frac{\Delta G}{4\pi R^2} = (\gamma_{12} - \gamma_{1w})(V_r + 1)^{-2/3} + \gamma_{2w} \qquad (6)$$

where $\Delta\psi$ is the free energy change per unit area of the overall composite particle.

Similar analysis were applied to other cases shown in Figure 1. The results are summarized in Table I. Eq. (10) is related to the volume of polymer 1 in the composite particle (case C in Fig. 1). Eq. (11) is based on the geometry of the triangle defined by angles θ and θ' in the same Figure. Eqs. (10) and (11) are solved simultaneously in order to calculate θ' and R_2/R. These values are then used in eq. (9) to calculate the surface energy for case C. Similar approach is used for hemisphere case C″ employing eqs. (13) and (14). Calculation of the free energy change using the equations listed in Table I involves a trial and error solution method. A WATFOR77 computer program was prepared for this purpose.

Table I Free Energy Changes Per Unit Area of the Overall Composite Particle for Various Morphological Structures of Latex Particles Dispersed in Water

Case	$\Delta\psi$ (Surface Energy/Area)	Equation No.
A (*core-shell*):	$(\gamma_{12} - \gamma_{1w})(V_r + 1)^{-2/3} + \gamma_{2w}$	(7)
A″ (*inverted core-shell*):	$(\gamma_{12} - \gamma_{1w} V_r^{-2/3})(V_r^{-1} + 1)^{-2/3} + \gamma_{1w}$	(8)
C (*hemisphere 1*):	$(1/2)\{(V_r + 1)^{-2/3}\gamma_{1w}(\cos\theta - 1) + (V_r + 1)^{-2/3}(1 - \cos\theta)\gamma_{12} + (R_2/R)^2(1 + \cos\theta')\gamma_{2w}\}$	(9)
	$(R_2/R)^3 = \{1 - (V_r + 1)^{-1}\{1 - (1/8)(1 - \cos\theta)[3\sin^2\theta + (1 - \cos\theta)^2]\}\}/\{1 - (1/8)(1 - \cos\theta')[3\sin^2\theta' + (1 - \cos\theta')^2]\}$	(10)
	$(R_2/R) = (V_r + 1)^{-1/3}\sin\theta/\sin\theta'$	(11)
C″ (*hemisphere 2*):	$(1/2)\{(R_1/R)^2(1 + \cos\theta')\gamma_{1w} + [\gamma_{12}(1 - \cos\theta) - 2\gamma_{1w}V_r^{-2/3}](V_r^{-1} + 1)^{-2/3} + (V_r^{-1} + 1)^{-2/3}(1 + \cos\theta)\gamma_{2w}\}$	(12)
	$(R_1/R)^3 = \{1 - (V_r^{-1} + 1)\{1 - (1/8)(1 - \cos\theta)[3\sin^2\theta + (1 - \cos\theta)^2]\}\}/\{1 - (1/8)(1 - \cos\theta)[3\sin^2\theta' + (1 - \cos\theta')^2]\}$	(13)
	$(R_1/R) = (V_r^{-1} + 1)^{-1/3}\sin\theta/\sin\theta'$	(14)
D (*individual particles*):	$\gamma_{2w}(V_r + 1)^{-2/3}V_r^{2/3}$	(15)

* Note that R_1 and R_2 are the radii of polymer 1 and polymer 2, respectively. θ or θ' (see Fig. 1) are the angles between the line which connects the two centers of the hemispheres and the other line which connects the centers and the three-phase point.

In applying any of the above approaches it will be necessary to have the corresponding values for the interfacial tensions of various phases measured under the prevailing polymerization conditions.

EXPERIMENTAL

Materials

Styrene monomer (Polyscience) was washed with 10% aqueous sodium hydroxide solution, followed by water, dried overnight (at 5°C) with anhydrous sodium sulfate (100 g/L) and passed through an activated aluminum oxide column to remove the inhibitor. Two monodisperse polystyrene latexes, LS 1121B and LS 1102A (Dow Chemical Co.) were used as seed. The PS latexes were cleaned by the serum replacement technique until the conductivity of the serum emerging from the filtration cell was close to that of DDI water. The monomers, methyl methacrylate, and ethyl methacrylate (Rohm and Haas Co.) were washed with 10% aqueous sodium hydroxide solution, followed by water, dried overnight (at 5°C) with anhydrous sodium sulfate (100 g/L) and vacuum distilled under dry nitrogen to remove the inhibitor. 2,2-Azobisisobutyronitrile initiator (Vazo 64, Du Pont Co.) was recrystallized twice from ethanol and then dried at room temperature in a vacuum oven. All other materials were used as received including potassium persulfate initiator ($K_2S_2O_8$, Fisher Scientific Co.), sodium bicarbonate buffer (Fisher Scientific Co.), Dowfax 3B2 surfactant diphenyloxide disulfonates, Dow Chemical Co.), Aerosol MA-80 emulsifier (sodium dihexyl sulfosuccinate, American Cyanamid Co.), Igepal Co-990 surfactant (nonylphenol polyethylene oxide, 100 moles ethylene oxide, GAF Co.), octane (reagent grade, Fisher Scientific Co.). Double-distilled deionized water was used in the preparation of aqueous solutions.

Seed Latex Preparation

Four polystyrene latex samples which differ in their particle surface polarity were characterized for use as seed latexes. Two were commercial monodisperse latexes, LS 1121B and LS 1102B (Dow Chemical Co.); the other two seed latexes (AI12 and KP28) were prepared using the recipes given in Table II. Batch emulsion polymerizations were carried out in rotating bottles at 70°C. The particle sizes of these latexes are measured by Coulter N4 or TEM.

Table II Polymerization Recipes

	AI12 (g)	KP28 (g)
DDI water	180	159.64
Styrene	90	40.35
AIBN	0.45	—
$K_2S_2O_8$	—	0.204
Aerosol MA-80	—	1.891
Dowfax 3B2 (15%)	10	—
$NaHCO_3$	0.27	0.252

Contact Angle Measurement

Contact angle of an octane drop at the latex "film"/water interface was used to estimate the polar component of surface tension of the latex film.[16] Octane/water/film interfaces were formed by immersing the latex film supported on a glass microslide in a glass observation cell containing octane-saturated water maintained at room temperature, and releasing octane drops beneath the film surface from a syringe. Since octane has a lower density than water the octane drops will float upward, touch the film surface, and form the interface. The advancing contact angles on both sides of each drop were recorded. A minimum of three drops were placed in series on each latex film, and at least three films of each polystyrene latex were used.

The polar component of the surface tension (γ^p) was calculated, using the harmonic mean equation approximation[17] described by Andrade et al.[18] for octane as the probe liquid

$$\gamma^p_{sv} = K_1\gamma^p_{wv}/(\gamma^p_{wv} - K_1) \quad (16)$$

where

$$K_1 = (\gamma_{ow}\cos\theta + \gamma_{wv} - \gamma_{ov})/4 \quad (17)$$

γ_{sv}, γ_{wv} and γ_{ov} are the surface tensions of the latex film, water, and octane, respectively; and γ_{ow} is the octane/water interfacial tension. Substituting γ_{ow} = 50.8 dyn cm^{-1},[19] γ^p_{wv} = 51.0 dyn cm^{-1},[19] γ_{wv} = 72.8 dyn cm^{-1},[19] and γ_{ov} = 21.8 dyn cm^{-1} [19] into eqns. (16) and (17) yields

$$\gamma^p_{sv} = 51.0(1.004 + \cos\theta)/(3.012 - \cos\theta) \text{ dyn cm}^{-1} \quad (18)$$

The surface polarity, X^p, of the latex particles was

estimated using the equation reported by Brouwer et al.[20] for polystyrene polymer

$$X^p = \gamma_{sv}^p/(39.15 + 0.66\gamma_{sv}^p) \qquad (19)$$

The latex "films" were prepared in the following manner. Latex was first cleaned by ion-exchange technique and then dried out at room temperature. The dried latex was pressed between two clean plastic Mylar films under 11,000 psi without heating. The films, 0.3 mm thick, were observed to be smooth and transparent.

Seeded Emulsion Polymerization and Particle Morphology

The composite latexes used in our morphology studies were prepared by batch seeded emulsion polymerization using Dow LS1102A (denoted as PS190), and Dow LS1121B (denoted as PS300) PS monodisperse particles as the seed particles. Two different acrylic monomers were used in the second stage polymerization, namely, methyl methacrylate and ethyl methacrylate. The second stage polymerization was carried out at 70°C in batch using magnetically stirred polymerization bottle. Table III gives the standard recipe used in the preparation of the two latex systems, PS190/PMMA-AIBN and PS300/PEMA-AIBN; nonionic initiator AIBN was used in both cases. The seed/monomer weight ratio was 30/70 for the PS190/PMMA-AIBN system and 40/60 for the PS300/PEMA-AIBN system. In one system, PS190/PMMA-KS, potassium persulfate (KS) was used as initiator in the second stage polymerization according to the recipe given in Table IV. The composite latexes were then cleaned by serum replacement until the refractive index of the serum emerging from the filtration cell was close to the DDI water. The particle morphology was observed by TEM after preferential staining of the polystyrene domains with RuO_4 vapor and negative staining with phosphotungstic acid (PTA) to better delineate the particle edges, especially for the methacrylate-rich domains, which are unstained by RuO_4.[14]

Table III Recipe of Seeded Emulsion Polymerization for PS190/PMMA-AIBN and PS300/PEMA-AIBN

Ingredients	Weight (g)
PS seed particles	1.0
Igepal Co-990	0.08
Monomer	Variable
DDI water	11.0
AIBN	0.005

Table IV Recipe of Seeded Emulsion Polymerization for PS190/PMMA-KS

Ingredients	Weight (g)
PS190	1
Igepal Co-990	0.08
DDI water	12.6
Methyl methacrylate	2.35
$K_2S_2O_4$	0.0118

Preparation of Homopolymer Latexes

Three homopolymer latexes—PEMA-AIBN, PMMA-AIBN, and PMMA-KS—were prepared in the absence of seed particles using the recipe given in Table V. In these polymerizations the initiator/monomer ratios and the polymerization temperature were the same as those used in the second stage polymerization used in the preparation of the composite latexes given in Tables III and IV. These homopolymer latexes are for use in the interfacial tension measurements representing the second stage polymer in the composite latexes. The latexes were first cleaned by ion-exchange technique and then dried out at room temperature before use.

Drop-Weight-Volume Method

The interfacial tension measurements of polymer/water interface at room temperature were done by drop-weight-volume method[21] for the following three systems. (1) Mutually saturated methyl methacrylate monomer (or ethyl methacrylate)/water interface; (2) System 1 with the addition of a small amount of non-ionic surfactant to the aqueous phase. For this purpose Igepal Co-990, in concentration of 0.8% by weight based on water was used in order to simulate the prevailing conditions during the second stage polymerization. (3) System 2, where a polymer PS (or PMMA) was added to the monomer phase in increased concentration while keeping the surfactant concentration in the aqueous phase unchanged.

Viscosity-Average Molecular Weight (M_v)

The viscosity-average molecular weight M_v, was measured using the Ubbelohde dilution viscometer

Table V Recipes for Homopolymer Latexes: Poly(Methyl Methacrylate) PMMA-KS, PMMA-AIBN, and Poly(Ethyl Methacrylate) PEMA-AIBN

	PMMA-KS (g)	PMMA-AIBN (g)	PEMA-AIBN (g)
DDI water	59.64	219.2	219.2
Methyl methacrylate	40.35	40	—
Ethyl methacrylate	—	—	40
Aerosol MA-80	1.4	4.8	4.8
$K_2S_2O_8$	0.204	—	—
AIBN	—	0.133	0.133
$NaHCO_3$	0.2522	—	—

at 25°C. Toluene and acetone were employed as solvents for polystyrene (PS) and poly(methyl methacrylate) (PMMA), respectively. The relationship between viscosity-average molecular weight and intrinsic viscosity is given by the following equations[33]

$$[\eta] = 1.7 \times 10^{-4} [M]^{0.69} \quad \text{(for PS-toluene)} \quad (20)$$

$$[\eta] = 0.75 \times 10^{-4} [M]^{0.7} \quad \text{(for PMMA-acetone)} \quad (21)$$

RESULTS AND DISCUSSION

Surface Polarity of Polystyrene Latex Particle

Table VI lists the mean contact angles of an octane drop at the latex film–water interface, the value of the polar component of the surface tension, γ_{sv}^p, calculated according to eq. (18), and the surface polarity, X^p, of the latex particles estimated using eq. (19).

The data for AI12 and KP28 indicate that latex AI12 produced using AIBN initiator, which should contain only weak polar OH end groups, has a much lower surface polarity by comparison to all other latexes, and is similar to that of the thermo-initiated polystyrene which does not contain any surface charges. The residual SO_4^- groups for the $K_2S_2O_8$ initiator substantially increased the surface polarity, as seen in sample KP28, as well as the Dow latexes.

Interfacial Tension of Polymer/Water Interface

The experimental results of polymer/water interfacial tension measurements as a function of polymer concentration for PS190 in MMA/water, PMMA-KS in MMA/water and PMMA-AIBN in MMA/water systems are given in Figure 2. Those for PS190 in EMA/water, PS300 in EMA/water, and PEMA-AIBN in EMA/water systems are given in Figure 3. The results of the interfacial tension measurements for every system showed that the interfacial tension first decreased and then remained constant, within the experimental error, as the polymer concentration increased. This is because the polar components of the polymer (e.g., polymer chains with SO_4^- end groups) are more surface active than the nonionic surfactant Igepal Co-990 and

Table VI Latex Surface Polarity Measured by Contact Angle Method

Latex	D_p (nm)	Contact Angle	γ_{sv}^p (dyn cm^{-1})	X^P
Dow LS 1121B (PS300)	309[a]	107	10.98	0.237
KP28	194[b]	113	9.19	0.203
Dow LS 1102A (PS190)	190[a]	113	9.19	0.203
AI12	222[b]	143.7	2.65	0.065
Polystyrene (thermal polymerization)	—	146.5	2.26	0.056
PEMA-AIBN	—	117.5	7.96	0.181

[a] Measured by TEM.
[b] Measured by Coulter N4.

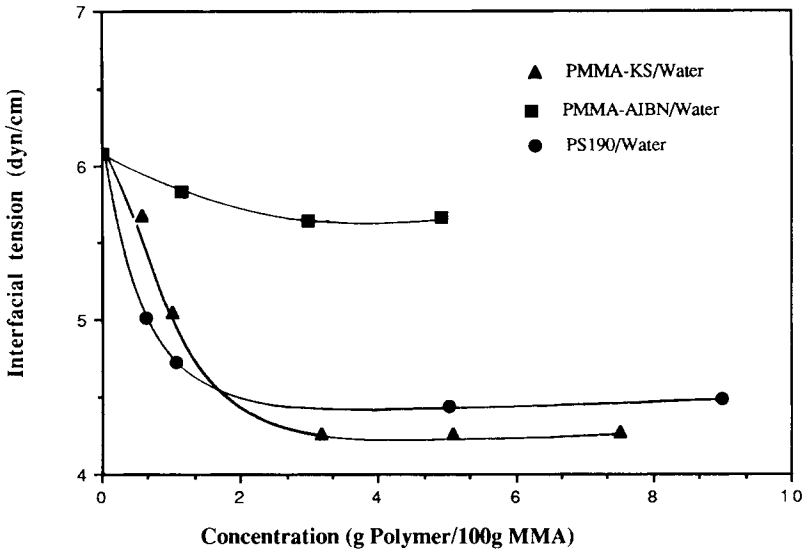

Figure 2 Interfacial tensions at 25°C for PS190 in MMA/water (●); PMMA-KS in MMA/water (▲); and PMMA-AIBN in MMA/water systems (■).

contribute to the decrease in interfacial tension. It seems that the sulfate or hydroxyl-containing polymer chains displace the surfactant at the interface thus increasing the polarity of the interface between polymer (in monomer) and water, until the polarity reaches a certain equilibrium point depending on the amount and nature of the polar components of the polymer. The data shown in Figure 2, suggest that the PMMA-KS latex with residual SO_4^- group from the $K_2S_2O_8$ initiator, which substantially increase the surface polarity of latex, decreased the interfacial tension more significantly than the PMMA-AIBN latex produced by using AIBN initiator, containing only weak polar groups.

Analyzing the interfacial tension data in Figure 3 and the surface polarity data in Table VI, one finds that the PS300 latex with the highest surface polarity, $X^P = 0.237$ ($\gamma^P = 10.98$ dyn/cm), in EMA to have a lower interfacial tension than PS190 latex with surface polarity, $X^P = 0.203$ ($\gamma^P = 9.19$ dyn/cm). For the case of PEMA-AIBN latex with surface polarity, $X^P = 0.181$ ($\gamma^P = 7.96$ dyn/cm), the in-

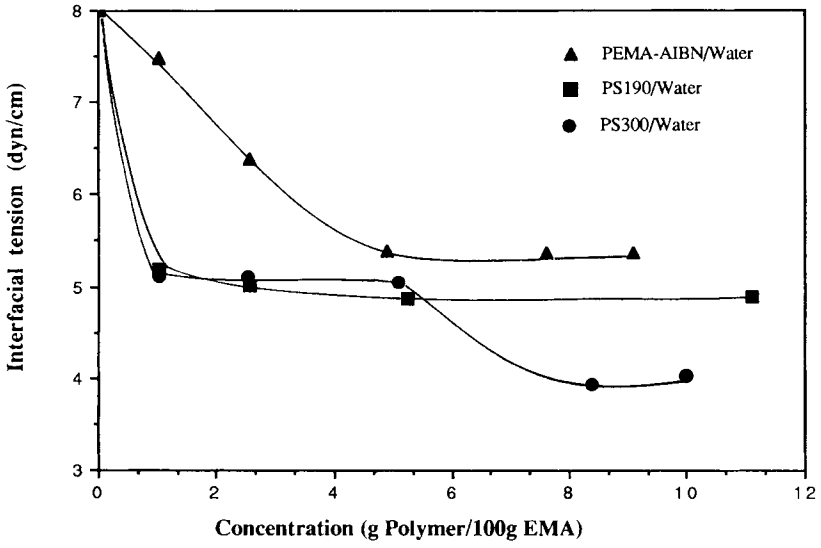

Figure 3 Interfacial tensions at 25°C for PS190 in EMA/water (■); PS300 in EMA/water (●); and PEMA-AIBN in EMA/water systems (▲).

terfacial tension is higher than both PS190 and PS300. These results showed that, rather than the polymer bulk hydrophilicity, the surface particle polarity is determined by the functional groups which result from the initiator fragments. These surface polarities of latex particles are key parameters in deciding which phase is inside or outside in composite particles. Polymers with the highest surface polarity and lower interfacial tension will favor to be on the outer surface of the composite latex particles. For example, based on the data presented in Figure 3, one can expect the final morphologies of the PS300/PEMA-AIBN composite latexes to be that of polystyrene domains on the surface of the PEMA. Indeed, the electron micrograph of these composite particles in Figure 4 shows that the lighter poly(ethyl methacrylate) is surrounded by the dark-stained polystyrene regions.

For the PS190 latex in different solvents, i.e., monomer MMA and EMA, different interfacial tension values were obtained (see Figs. 2 and 3). This indicates that the use of nonpolymerizable additives to change the oil phase property, e.g., a second solvent miscible with monomer, could be an approach to influence the interfacial tension, and therefore, the final morphology of the composite particle.

Interfacial Tension of Polymer 1/ Polymer 2 Interface

For the estimation of interfacial tension between polymer 1/polymer 2 under the prevailing polymerization conditions, the phenomenon can be approached as a solution of the two polymers in a mutual solvent, i.e., the second stage monomer. Usually a liquid–liquid phase separation occurs even at low polymer concentration. The interfacial properties of such demixed systems have been investigated in recent years. All the experiments and theories were concerned mainly with the interfacial tension and the thickness of the interfacial layer, especially with respect to their dependence on the molecular weight of the polymer chains, the monomer concentration, and the temperature. However, only a few reports on the direct measurement of the interfacial tension in the ternary systems were published[22–24]; all those measurements were confined to dilute polymer solutions. In addition, the different theories proposed so far also yield rather controversial results. Most of these calculations are based essentially on the mean field type approach developed for polymer mixtures, i.e., they are derived from a Flory–Huggins expression for free energy[25] or from self-consistent field models.[26,27] However, these mean field theories did not consider the effects of the excluded volume,[28] which are very important in polymer solutions. Recently, Broseta et al.[29] proposed a theory of interfacial tension and concentration profiles taking into account the excluded volume effect. They measured the interfacial tension of demixed poly(styrene)–poly(dimenthylsiloxane) mixtures dissolved in toluene as a function of molecular weight of polymers and monomer concentration. A very good agreement between the experimental results and the theoretical

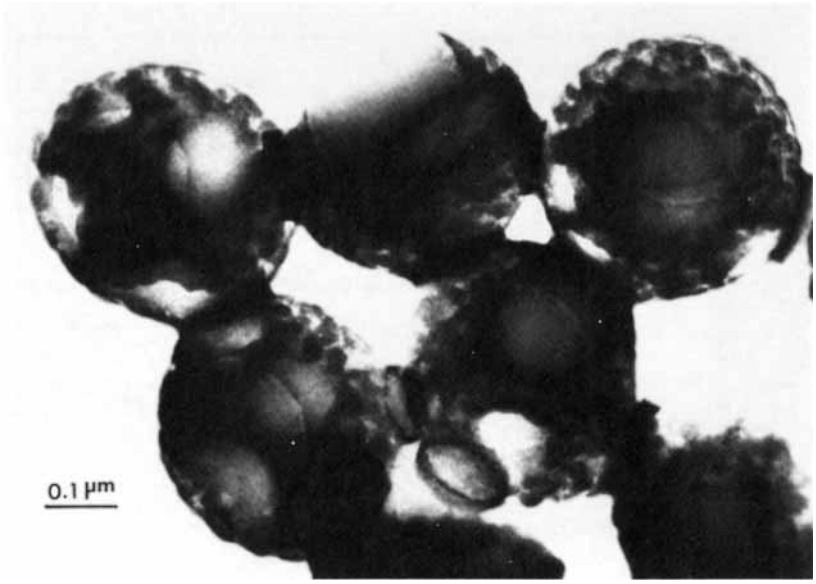

Figure 4 TEM of PS300/PEMA-AIBN composite polymer particle with 40/60 weight seed to shell ratio. Dark regions are polystyrene stained with RuO_4 and lighter regions are acrylate domains outlined using phosphotungstic acid stain.

predictions was reported. Broseta's approach was applied in estimating the interfacial tensions of the PS190/PMMA-AIBN and PS190/PMMA-KS systems, making use of the following equations

$$\gamma = \gamma_o[1 - 1.64/\omega - 1.67u] \quad (22)$$

where

$$\gamma_o = kT(u/6)^{1/2}/\xi^2 \quad (23)$$

ξ is the correlation length of semidilute polymer solutions, which depends on the concentration according to the universal law[30]

$$\xi(c)/Rg = 0.43(c/c^*)^{-3/4} \quad (24)$$

where c^* is the overlap concentration (at which the chains begin to overlap), which can be expressed as

$$c^* = 3M/4\pi Rg^3 N_{AV} \quad (25)$$

u is the interaction parameter between unlike "blobs",[28] which can be estimated from the knowledge of the critical concentration of demixing c_k in the semidilute regime

$$u(c) = u_o(c/c_k)^{0.3} \quad (26)$$

The critical concentration is given by the following equation[29]

$$u_o = 2c_k\xi_k^3/M \quad (27)$$

where ω is the incompatability degree, which can be expressed as

$$\omega = uN_b \quad (28)$$

Here,

$$N_b = M/c\xi^3 \quad (29)$$

represents the number of blobs per chain. M is the averaged molecular weight of both polymers. By using eqs. (22)-(29), the interfacial tension can be estimated in terms of measurable quantities such as molecular weight M, radius of gyration of chains in

Table VII Molecular Weight and Radius of Gyration of PS190, PMMA-AIBN, and PMMA-KS

Sample	M_v[a]	Rg (Å)	c_k (10^2 g/cm^3)[d]
SI PS190	8.4×10^5	409[b]	5.29
PMMA-KS	14.6×10^5	877[c]	
SII PS190	8.4×10^5	409[b]	3.85
PMMA-AIBN	26.3×10^5	1239[c]	

[a] M_v is viscosity-average molecular weight of PMMA in acetone or PS in toluene.
[b] Ref. 32.
[c] From the measurement of relative viscosities of solution.
[d] By solving the following equations:

$$c_k = 227\, M^{-0.61}$$

$$V = \frac{W_{PS}}{\rho_{PS}} + \frac{W_{PMMA}}{\rho_{PMMA}} + \frac{100\text{ g} - (W_{PS} + W_{PMMA})}{\rho_{MMA}}$$

$$c_k = \frac{W_{PS} + W_{PMMA}}{V}$$

$$M = \frac{W_{PS} \times (M_v \text{ of PS190}) + W_{PMMA} \times (M_v \text{ or PMMA})}{W_{PS} + W_{PMMA}}$$

where

M: the (weight) average molecular weights of PS190 and PMMA chains; V: volume of polymer solution (PS and PMMA in MMA); W_{PS}: weight of PS190; W_{PMMA}: weight of PMMA; ρ_{PS}: density of PS; ρ_{PMMA}: density of PMMA; and ρ_{MMA}: density of MMA monomer.

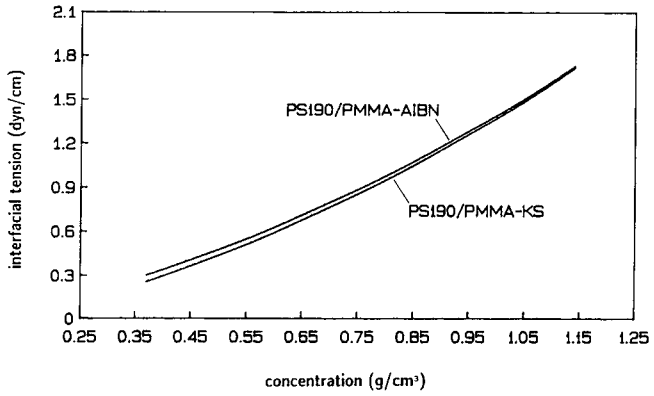

Figure 5 Calculated interfacial tension of 30/70 weight ratio of polymer 1/polymer 2 systems of PS190/PMMA-AIBN and PS190/PMMA-KS as a function of polymer concentration in MMA monomer.

the dilute solution Rg, and critical concentration of demixing c_k. A WATFOR77 computer program was prepared for this purpose. Table VII gives the molecular weight and radius of gyration of PS190, PMMA-KS, and PMMA-AIBN. The critical concentration of demixing, c_k, for PS/PMMA/MMA ternary system was not reported previously, but the c_k for PS/PMMA/Benzene system is available as given by the following equation[31]

$$c_k = 277M^{-0.61} \tag{30}$$

Eq. (30) was employed because of the similarity of the thermodynamic properties of benzene and MMA (the parameters $k = 0.3934$ and $a = 0.7627$ of the Mark–Houwink equation $[\eta] = kM^a$ for PMMA in MMA at 25°C are close to those of PMMA in benzene, $k = 0.55$ and $a = 0.76$).

Figure 5 gives the calculated results for the dependence of the interfacial tension between both phases of the demixed ternary mixtures PS190/PMMA-AIBN/MMA or PS190/PMMA-KS/MMA on the overall polymer concentration, for a final polymer 1/polymer 2 ratio of 30/70. The increase in the interfacial tension as the polymer concentration is increased indicates that the interfacial tension would also increase during the course of emulsion polymerization as the conversion is increased. Therefore, the tendency of phase separation of polymer phases in the composite latex during the course of seeded emulsion polymerization is also expected to increase. In addition, by comparing the interfacial tensions of these two ternary mixtures, the polymer with the lower molecular weight (see Table VII for PS190/PMMA-KS system) results in lower interfacial tension. These results reveal that controlling the molecular weight by using a chain transfer agent in seeded emulsion polymerization could be a way to change the morphology of the composite latex particles.

Results of Model Prediction and Discussion

Based on the estimated interfacial tensions, the composite particle configurations of the PS190/PMMA-AIBN and PS190/PMMA-KS systems at

Table VIII Configurations of PS190/PMMA-AIBN System at 30/70 Polymer Weight Ratio

PS190/PMMA-AIBN			Configurations at 10% Conversion		Final Configurations		
Weight Ratio	γ_{1w}[a]	γ_{2w}[a]	γ_{12}[b]	Case Predicted	γ_{12}[c]	Case Predicted	Observed
30/70	4.46	5.66	0.30	A″	1.50	C″ $\theta = 92°$	C″

[a] From Figure 2.
[b] From Figure 5, at 10% conversion (= 0.37 g/cm³ on x-axis).
[c] From Figure 5, at 90% conversion (= 1.05 g/cm³ on x-axis).

30/70 polymer/polymer weight ratio were predicted by using the equations listed in Table I. The calculation of the free energy change for each case was done by a WATFOR77 computer program. The predicted composite particle morphology is the one which has the minimum free energy change. The results are given in Tables VIII and IX.

The last two columns of Tables VIII and IX show the predicted and observed configurations. For the PS190/PMMA-AIBN system at the 30/70 weight ratio, the predicted morphology was case C″ (see Fig. 1) with θ angle 92°. The morphology of the composite latex is shown in Figure 6. The electron micrographs in Figure 6 show that the second stage polymer PMMA (lighter region) is partially engulfed by the seed polystyrene (darker region). This is more evident in the micrograph in Figure 6(B) where as a result of the electron beam damage during

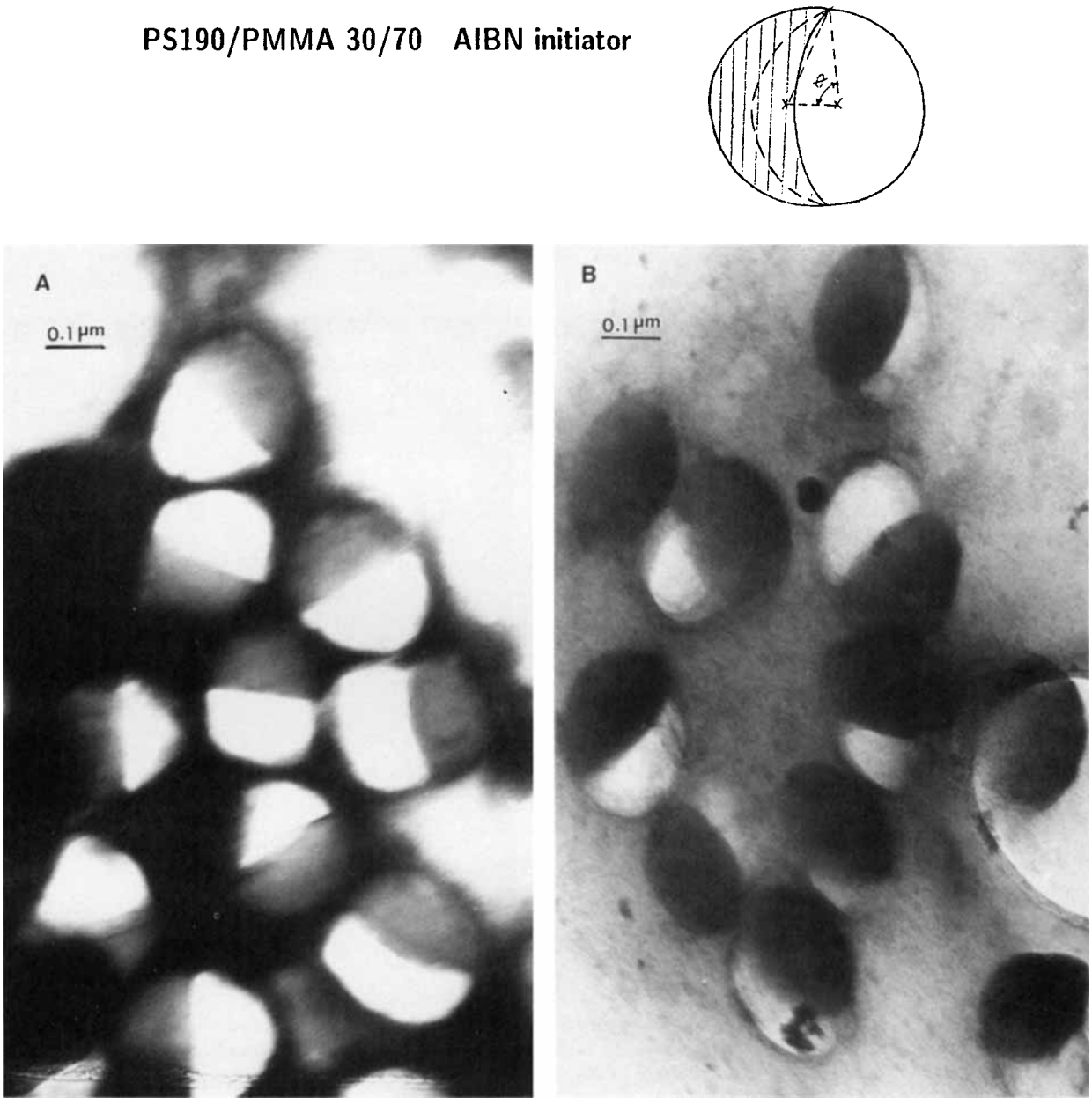

Figure 6 (A) TEM of seed PS190/PMMA-AIBN composite latex with 30/70 weight ratio. (B) As PMMA was damaged by electron beam, the cap shape of PS190 was observed. Dark regions are PS domains stained with RuO_4 and lighter regions are PMMA domains outlined using phosphotungstic acid stain.

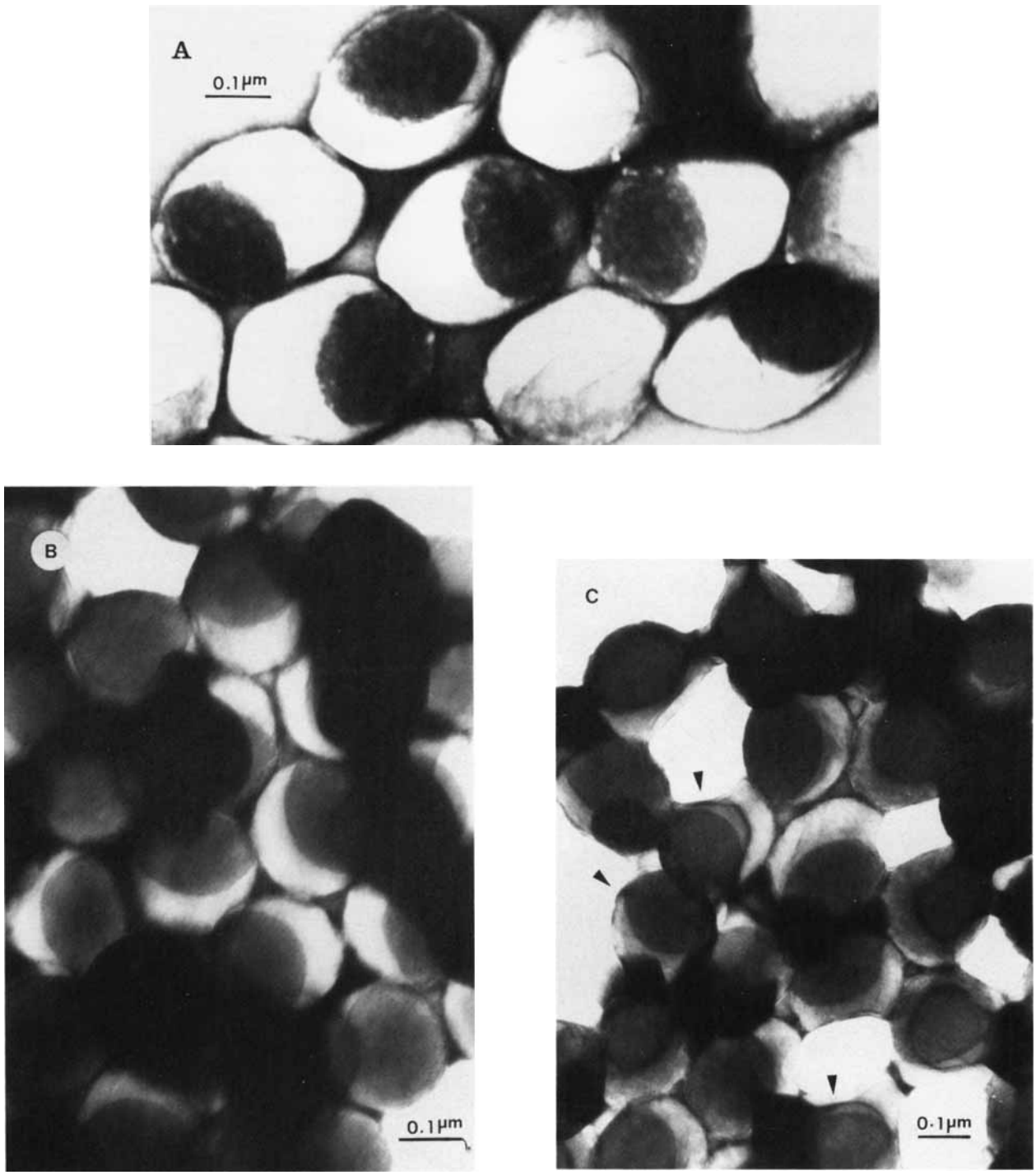

Figure 7 (A) and (B) TEM of PS190/PMMA-KS composite latex with 30/70 weight ratio. Dark regions are PS domains stained with RuO_4 and lighter regions are PMMA domains outlined using phosphotungstic acid stain. (C) As the PMMA was damaged by electron beam (▶), the spherical shape of PS190 was observed. Dark regions are PS domains stained with RuO_4 and lighter regions are PMMA domains outlined using phosphotungstic acid stain.

Table IX Configurations of PS190/PMMA-KS System at 30/70 Polymer Weight Ratio

PS190/ PMMA-KS			Configurations at 10% Conversion		Final Configurations		
Weight Ratio	γ_{1w}[a]	γ_{2w}[a]	γ_{12}[b]	Case Predicted	γ_{12}[c]	Case Predicted	Observed
30/70	4.46	4.26	0.25	C $\theta = 153°$	1.48	C $\theta = 89°$	C

[a] From Figure 2.
[b] From Figure 5, at 10% conversion (= 0.37 g/cm^3 on x-axis).
[c] From Figure 5, at 90% conversion (= 1.05 g/cm^3 on x-axis).

TEM observation the PMMA domains shrunk and the cap shape of polystyrene domains is easier to see. The particle morphology in Figure 6 corresponds well to its schematic representation case C″ in Figure 1 based on the predicted θ angle in which the polystyrene domain appear as a cap partially covering the PMMA domains. The same good agreement of the experimental results with the theoretical predictions was also obtained for the PS190/PMMA-KS system. Figure 7 clearly shows that case C is prevailing, where now the PMMA lighter regions are partially covering the polystyrene darker regions. Figure 7(C) shows the case where the composite particles were not fully embedded in PTA (particles marked by arrows); the PMMA domains suffered beam damage which allowed the spherical shape of the PS core to be observed. Thus the use of $K_2S_2O_8$ as initiator in the second stage polymerization resulted in allowing the second stage PMMA to partially engulf the original polystyrene seed particles.

The usefulness of the thermodynamic calculations to predict the "equilibrium" morphology is obvious. Hence, these results encouraged us to predict the particle morphology at a lower percent conversion, which we choose as 10%. The results are given in Tables VIII and IX. For PS190/PMMA-AIBN system, prediction of case A″ (inverted core–shell) was obtained. The change in morphology from case A″ (inverted core–shell) at low conversion to case C″ (hemisphere 2) for the final configuration indicates an increase in the extent of phase separation during the polymerization. The same tendency has been found in the PS190/PMMA-KS system. Although the predicted morphology at 10% conversion, case C, is the same as that of the final latex, the decrease in θ angle from 153° to 89° as the polymerization increased indicates an increase in phase separation. This is attributed to the increase in the polymer 1/polymer 2 interfacial tension as the polymerization proceeds due to the increased polymer concentration as shown in Figure 5.

In order to evaluate the influence of the interfacial tension of each polymer at the polymer 1/polymer 2 interface as well as the polymers volume ratio (V_r) on the final composite particle morphology, a number of hypothetical conditions corresponding to various values of γ_{ij} and V_r have been used in the calculations for minimizing the free energy of the system. The selected values of these parameters and the predicted morphologies are summarized in Table X.

A comparison of the data in groups 1 and 2 shows that one expects a higher chance of obtaining the

Table X Various Morphological Structures of Latex Particles Dispersed in Water Under Hypothetical Conditions

Group	γ_{1w}	γ_{2w}	γ_{12}	V_r	Case Predicted*
1	9	5	3	1	A
	5	9	3	1	A″
2	7	5	3	1	C $\theta = 86°$
	5	7	3	1	C″ $\theta = 86°$
3	9	5	4.1	1	C $\theta = 134°$
	9	5	6	1	C $\theta = 70°$
	9	5	8	1	C $\theta = 53°$
	9	5	10	1	C $\theta = 40°$
	9	5	15	1	D
	5	9	4.2	1	C″ $\theta = 119°$
	5	9	7	1	C″ $\theta = 61°$
	5	9	9	1	C″ $\theta = 46°$
	5	9	15	1	D
4	9	5	4.5	0.5	C $\theta = 86°$
	9	5	4.5	1.5	C $\theta = 109°$
	9	5	4.5	2.5	C $\theta = 118°$
	9	5	4.5	3.5	C $\theta = 124°$
	9	5	4.5	5.5	C $\theta = 129°$
	5	9	4.5	0.5	C″ $\theta = 114°$
	5	9	4.5	1.5	C″ $\theta = 93°$
	5	9	4.5	2.5	C″ $\theta = 81°$
	5	9	4.5	5.8	C″ $\theta = 65°$

* See Figure 1 for schematic representation of morphology.

desired core–shell morphology (case A) if the interfacial tensions between the seed polymer and water is higher than that between the second stage polymer and water (i.e., $\gamma_{1w} \gg \gamma_{2w}$). On the other hand, one only has to allow γ_{2w} to be greater than γ_{1w} in order to invert the particle morphology (case A″). Analyzing the data in groups 1 and 3, one finds that as the polymer 1/polymer 2 interfacial tension (γ_{12}) increases while maintaining the γ_{1w}, γ_{2w}, and V_r constant, the equilibrium particle morphology changes from case A (or A″) to case C (or C″), and finally to case D (individual particles). This phenomenon of the increase in the phase separation as γ_{12} is increased indicates that the γ_{12} is a parameter which decides the interfacial area between the two polymer phases. The data in group 4 show how the volume ratio of the second stage polymer to the seed polymer affects the particle morphology. If γ_{1w} is greater than γ_{2w}, the tendency of decreasing phase separation can be enhanced by increasing the volume ratio, as indicated by the increase in θ (86°–129°) while V_r is increased from 0.5 to 5.5. On the contrary, if γ_{2w} is greater than γ_{1w}, increasing of the volume ratio V_r in the range of 0.5 to 5.8 should result in an increase in the tendency of phase separation as indicated by the decrease in θ from 114° to 65°. Experimental data are still required in order to confirm these predictions.

CONCLUSIONS

Polystyrene latex produced using AIBN initiator which contains only weak polar surface groups results in particles with low surface polarity. The polystyrene latex particles with residual SO_4^- groups from the $K_2S_2O_8$ initiator can acquire a substantially high surface polarity, depending on the amount of SO_4^- on the particle surface.

Particles with low surface polarity cause the polymer solutions in the second stage monomer to have a relatively high interfacial tension vs. the aqueous phase. Therefore, the particle surface polarity could be the controlling parameter in deciding which phase is inside or outside in composite particles, rather than the polymer bulk hydrophilicity.

The polymer 1/polymer 2 interfacial tension would increase during the course of seeded emulsion polymerization. This can cause an increase in the tendency of phase separation of the composite particle.

Based on the interfacial tensions, the predicted morphologies showed quite a good agreement with the observed particle morphologies of the composite latexes. These results proved that the interfacial tension is one of the main parameters controlling particle morphology in composite latexes.

REFERENCES

1. P. I. Lee, in *Emulsion Polymers and Emulsion Polymerization*, D. R. Bassett and A. E. Hamielec, Eds.; ACS Symp. Ser., No. 165, 1981, p. 405.
2. T. T. Min, A. Klein, M. S. El-Aasser, and J. W. Vanderhoff, *J. Polym. Sci. Polym. Chem. Ed.*, **21,** 2845 (1983).
3. D. J. Hourston, R. Satgurunthan, and H. Varamn, *J. Appl. Polym. Sci.*, **31,** 1955 (1986) and **33,** 215 (1987).
4. I. Cho and K. W. Lee, *J. Appl. Polym. Sci.*, **30,** 1903 (1985).
5. S. Muroi, H. Hashimoto, and K. Hosoi, *J. Polym. Sci. Polym. Chem. Ed.*, **22,** 1365 (1984).
6. D. I. Lee and T. Ishikawa, *J. Polym. Sci. Polym. Chem. Ed.*, **21,** 147 (1983).
7. D. R. Stutman, A. Klein, M. S. El-Aasser, and J. W. Vanderhoff, *Ind. Engr. Chem. Prod. Res. Dev.*, **24,** 404 (1985).
8. M. Okubo, Y. Katsuta, and T. Matsumoto, *J. Polym. Sci. Polym. Lett. Ed.*, **18,** 481 (1980).
9. M. Okubo, A. Yamada, and T. Matsumoto, *J. Polym. Sci. Polym. Chem. Ed.*, **16,** 3219 (1980).
10. M. Okubo, Y. Katsuta, and T. Matsumoto, *J. Polym. Sci. Polym. Lett. Ed.*, **20,** 45 (1982).
11. M. Okubo, M. Ando, A. Yamada, Y. Katsuta, and T. Mastsumoto, *J. Polym. Sci. Polym. Lett. Ed.*, **19,** 143 (1981).
12. J. Berg, D. Sundberg, and B. Kronberg, *Polym. Mater. Sci. Engrg.*, **54,** 367 (1986).
13. D. C. Sundberg, 19th Annual Short Course, *Advances in Emulsion Polymerization and Latex Technology*, June 6–10, 1988, Emulsion Polymers Institute, Lehigh University.
14. V. L. Dimonie, M. S. El-Aasser, and J. W. Vanderhoff, *Polym. Mater. Sci. Engrg.*, **58,** 821 (1988).
15. S. Torza and S. Mason, *J. Colloid Interface Sci.*, **33,** 67 (1970).
16. W. C. Hamilton, *J. Colloid Interface Sci.*, **40,** 219 (1972).
17. S. Wu, *J. Macromol. Sci. Rev. Macromol. Chem.*, **C10,** 1 (1974).
18. J. D. Andrade, S. M. Ma, R. N. King, and D. E. Gregonis, *J. Colloid Interface Sci.*, **72,** 488 (1979).
19. J. T. Davies and E. K. Rideal, *Interfacial Phenomena*, 2nd Ed., Academic, New York, 1987, p. 2.
20. W. M. Brouwer and R. L. J. Zsom, *Colloids and Surfaces*, **24,** 195 (1987).
21. J. L. Lando and H. T. Oakley, *J. Colloid Interface Sci.*, **25,** 526 (1967).
22. G. Langhammer and L. Nestler, *Makromol. Chem.*, **88,** 179 (1965).

23. G. Riess, *Makromol. Chem. Rapid. Commun.*, **1,** 771 (1980).
24. K. Shinozaki, Y. Satio, and T. Nose, *Polymer*, **23,** 1937 (1982).
25. A. Vrij, *J. Polym. Sci.*, **A-2,** 6, 1919 (1968); A. Vrij and G. J. Roebersen, *J. Polym. Sci., Polym. Phys. Ed.*, **15,** 109 (1977).
26. E. Helfand and Tagami, *J. Chem. Phys.*, **56,** 3592 (1972); **57,** 1812 (1972); *J. Polym. Sci.*, **B9,** 741 (1971); E Helfand and A. M. Sapse, *J. Chem. Phys.*, **62,** 1327 (1975).
27. K. M. Hong and J. Noolandi, *Macromolecules*, **13,** 964 (1980); **14,** 736 (1981).
28. On scales larger than ξ, chains are ideal and excluded-volume interactions are screened out. Because the screening effects the chains may be viewed as a succession of uncorrelated subunits (blobs). Each blob occupies the correlation volume ξ^3. u denotes the effective interactive parameter between unlike blobs. See: D. Broseta, L. Leibler, and J. F. Joanny, *Macromolecules,* **20,** 1935 (1987).
29. D. Broseta and L. Leibler, *J. Chem. Phys.*, **87,** 7248 (1987).
30. A. Lapp, C. Picot, and C. Strazielle, *J. Phys. Lett.*, **46,** L1031 (1985).
31. L. Ould Kaddour, I. Soleda Anasagati, and C. Strazielle, *Makromol. Chem.*, **188,** 2223 (1987).
32. J. Cotton, *J. Phys. Lett.*, **41,** L231 (1980).
33. M. Kurata, M. Iwawa, and K. Kamada, in *Viscosity-Molecular Weight Relationships and Unperturbed Dimensions of Linear Chain Molecules*, J. Brandrup and E. H. Immergut, Eds., with the collaboration of H.-G. Elias, Polymer Handbook, Interscience Div., Wiley, New York, 1966, pp. IV-1–IV-72.

Received Ocotober 20, 1989
Accepted April 23, 1990